2020-09

TWO CANTED MEMS ACOUSTIC SENSORS FOR FINDING DIRECTION IN UNDERWATER

Park, Kwangjun

Monterey, California. Naval Postgraduate School

NAVAL POSTGRADUATE SCHOOL

MONTEREY, CALIFORNIA

THESIS

TWO CANTED MEMS ACOUSTIC SENSORS FOR FINDING DIRECTION IN UNDERWATER

by

Kwangjun Park

September 2020

Thesis Advisor: Gamani Karunasiri
Co-Advisor: Renato Rabelo

THIS PAGE INTENTIONALLY LEFT BLANK

REPORT DOCUMENTATION PAGE	*Form Approved OMB No. 0704-0188*

1. AGENCY USE ONLY *(Leave blank)*	**2. REPORT DATE** September 2020	**3. REPORT TYPE AND DATES COVERED** Master's thesis

4. TITLE AND SUBTITLE
TWO CANTED MEMS ACOUSTIC SENSORS FOR FINDING DIRECTION IN UNDERWATER

5. FUNDING NUMBERS

6. AUTHOR(S) Kwangjun Park

7. PERFORMING ORGANIZATION NAME(S) AND ADDRESS(ES)
Naval Postgraduate School
Monterey, CA 93943-5000

8. PERFORMING ORGANIZATION REPORT NUMBER

9. SPONSORING / MONITORING AGENCY NAME(S) AND ADDRESS(ES)
N/A

10. SPONSORING / MONITORING AGENCY REPORT NUMBER

11. SUPPLEMENTARY NOTES The views expressed in this thesis are those of the author and do not reflect the official policy or position of the Department of Defense or the U.S. Government.

12a. DISTRIBUTION / AVAILABILITY STATEMENT
Approved for public release. Distribution is unlimited.

12b. DISTRIBUTION CODE
A

13. ABSTRACT (maximum 200 words)

Micro electromechanical system (MEMS)-based acoustic sensors can be operated in the pressure gradient mode to obtained direction of underwater sound. A single MEMS sensor is unable to resolve left and right ambiguity due to cosine directional response. However, recent measurements carried out in air using two such sensors mounted at a canted angle allowed the determination of baring of sound unambiguously. In this thesis, the work carried out in air will be extended for applications in underwater by using two canted MEMS sensors packaged operate in an underwater environment. The canted system will be characterized in an anechoic chamber with and without underwater packaging and then using the NPS water tanks. The measurements include frequency and directional responses to determine their ability of operating in an underwater environment to accurately obtaining the bearing of sound.

14. SUBJECT TERMS
MEMS, underwater, sensor, canted, acoustic

15. NUMBER OF PAGES
55

16. PRICE CODE

17. SECURITY CLASSIFICATION OF REPORT	**18. SECURITY CLASSIFICATION OF THIS PAGE**	**19. SECURITY CLASSIFICATION OF ABSTRACT**	**20. LIMITATION OF ABSTRACT**
Unclassified	Unclassified	Unclassified	UU

NSN 7540-01-280-5500

Standard Form 298 (Rev. 2-89)
Prescribed by ANSI Std. 239-18

THIS PAGE INTENTIONALLY LEFT BLANK

Approved for public release. Distribution is unlimited.

TWO CANTED MEMS ACOUSTIC SENSORS FOR FINDING DIRECTION IN UNDERWATER

Kwangjun Park
Lieutenant, Republic of Korea Navy
BA, ROK Naval Academy, 2011

Submitted in partial fulfillment of the
requirements for the degree of

MASTER OF SCIENCE IN ENGINEERING ACOUSTICS

from the

NAVAL POSTGRADUATE SCHOOL
September 2020

Approved by: Gamani Karunasiri
Advisor

Renato Rabelo
Co-Advisor

Oleg A. Godin
Chair, Department of Physics

THIS PAGE INTENTIONALLY LEFT BLANK

ABSTRACT

Micro electromechanical system (MEMS)-based acoustic sensors can be operated in the pressure gradient mode to obtained direction of underwater sound. A single MEMS sensor is unable to resolve left and right ambiguity due to cosine directional response. However, recent measurements carried out in air using two such sensors mounted at a canted angle allowed the determination of baring of sound unambiguously. In this thesis, the work carried out in air will be extended for applications in underwater by using two canted MEMS sensors packaged operate in an underwater environment. The canted system will be characterized in an anechoic chamber with and without underwater packaging and then using the NPS water tanks. The measurements include frequency and directional responses to determine their ability of operating in an underwater environment to accurately obtaining the bearing of sound.

THIS PAGE INTENTIONALLY LEFT BLANK

TABLE OF CONTENTS

LIST OF FIGURES

LIST OF ACRONYMS AND ABBREVIATIONS

DI	directivity index
DF	direction finding
ILD	interaural level difference
ITD	interaural time difference
MEMS	micro electromechanical system
NPS	Naval Postgraduate School
PCBs	printed circuit boards
SOIMUMPS	silicon-on-insulator multi-user manufacturing process
SRL	Sensor Research Lab
TRANSDEC	Transducer Evaluation Center
UW	underwater

THIS PAGE INTENTIONALLY LEFT BLANK

ACKNOWLEDGMENTS

First of all, I thank the Republic of Korea Navy and Naval Postgraduate School for giving me this opportunity. My purpose of studying here is to improve the Anti-Submarine warfare ability of Republic of Korea Navy. It has been a difficult time to live and study here. But, thanks to U.S. and international students' help, I can do all.

Professor Gamani Karunasiri, my advisor; Dr. Fabio Alves; and Dr. Renato Rabelo have given incredible intellectual stimuli for understanding and finishing my project. I pay tribute to their dedication and passion and support. Thanks to their efforts, I'm able to think critically and improve on the understanding of physics and mathematics.

To the professors and technical staff in the Physics and Engineering Acoustics departments—Dr. Bruce Denardo, Dr. Peter Crooker, Steven Jacob, Jeff Catterlin, and Jay Adeff—thank you for your sacrifice and knowledge. Also, I am grateful to my teammates in SRL, Jason Roberts, Brian Gureck, and Leland Mccarty.

I'd like to thank my beloved wife, Seonyeong Ha, for stopping her job for a while and sacrificing for her family. Thanks to your sacrifice, I'm able to finish my studies and projects. And to my kids, Juseong and Juha, I love you.

THIS PAGE INTENTIONALLY LEFT BLANK

I. INSTRUCTIONS

A. BACKGROUND

Many studies have been done to determine how humans and animals find the direction of a sound. The early investigations done by J. B. Venturi in 1796 found that humans employ the inequality of two impression by their two ears [1]. Later studies by Lord Rayleigh concluded that the difference in distance that sound travels between the two ears caused an amplitude difference which is used for determining the direction [2]. The auditory system was found to recognize the direction using the difference in strength at high frequencies and the arrival time difference at low frequencies [2]. Thus, the interaural time difference (ITD) and the interaural level difference (ILD) play an important role in finding the direction of a sound. More recent studies found that smaller size creatures employ a different approach to finding the direction of sound due to negligibly small ITD and ILD. For example, the female *Ormia Ochracea* fly uses its unique hearing organ to locate chirping crickets in order to lay eggs on them. The distance of the parasitic fly's eardrums is about 1.5 mm, while its host emits sound with 4.8 kHz having 70 mm wavelength. The distance between eardrums is too short to use conventional approaches for accurately determining the direction of sound. The hearing system of the fly has evolved for increasing ITD and ILD before the sound signal is transmitted to the central nervous system achieving about 2^o directional accuracy [3]. There have been many attempts to develop a sensor based on the fly's hearing system [4-16].

The Sensor Research Lab (SRL) at Naval Postgraduate School (NPS) began research in 2006 to use the characteristics of the fly's hearing organ to develop a directional sound sensor. The sensors were initially developed to operate in air and fabricated using micro electrical mechanical system (MEMS) technology. A typical sensor consists of two wings connected by a bridge that is similar to that of the fly's coupled eardrums. The entire mechanical structure is connected to a substrate using two torsional legs.

Figure 1 shows a micrograph of a sensor fabricated using silicon-on-insulator multi-user manufacturing process (SOIMUMPs) developed by the MEMSCAP foundry service [17]. The details of the sensor fabrication and characterization can be found in [18].

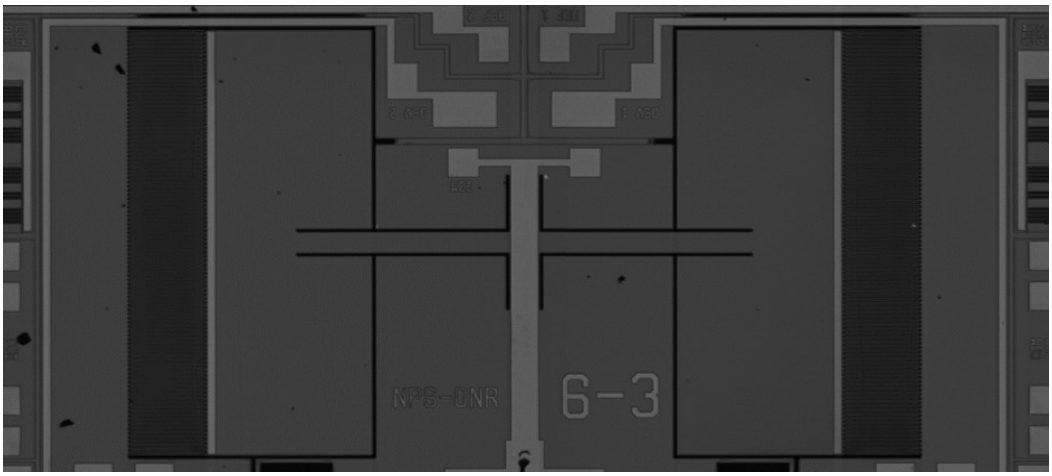

Figure 1. Previous generation MEMS acoustic DF sensor. Source: [19].

Figure 2 (a) depicts the measured frequency response of the sensor in air with sound incident at 45^{o} showing two resonant peaks at 1250 Hz and 1600 Hz. The two resonant peaks originated from the rocking and bending natural modes of the mechanical structure of the sensor [20]. The rocking mode has a smaller amplitude since it is excited by the pressure difference between the two wings generated by the incident sound wave. The bending mode has a larger amplitude since the full pressure of the incident sound wave generates it [20]. In addition, the sensor exhibited cosine dependence to the incident direction of sound when measured at the bending resonant frequency as shown in Figure 2 (b). This behavior arose from the sound interaction from front and back sides of the sensor which acts like a pressure gradient microphone [21].

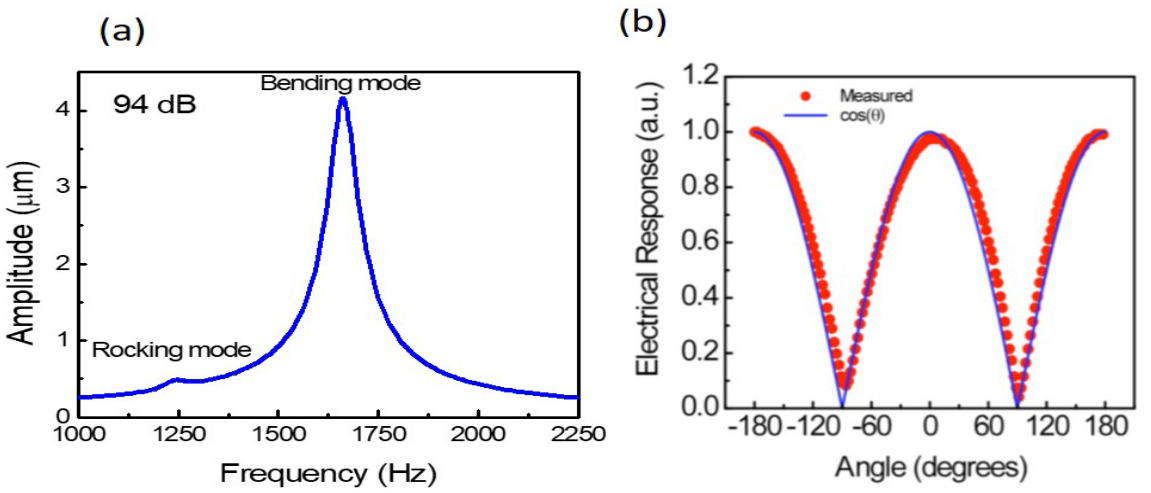

Figure 2. Frequency response (a) and directional response (b). Source: [18].

In early studies, researchers tried to find the direction of a sound using a single MEMS directional sound sensor. When operated at the bending resonance, a single sensor showed a symmetric response around the normal as shown in Figure 2 (b) which makes the determination of the direction ambiguous. To overcome this problem, two canted sensors were used to find the direction of arrival of sound as shown schematically in Figure 3 [22].

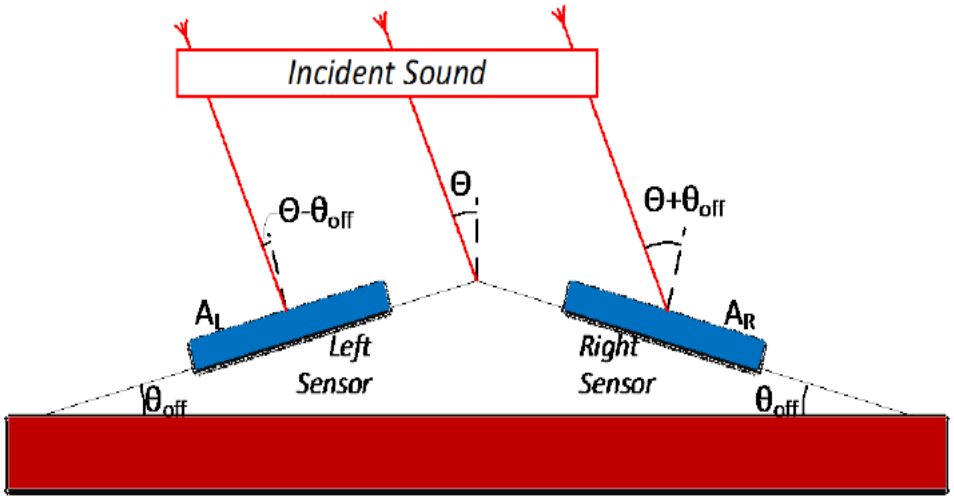

Figure 3. The schematics of two canted sensor assembly. Source: [22].

Left and Right sensors are located at offset angle, θ_{off} . They receive approximately the same pressure amplitude P_0 from a sound source with incident angles, $\theta-\theta_{off}$ (left) and $\theta+\theta_{off}$ (right) making them produce different outputs, P_L and P_R that be written as [9]:

$$P_L = P_0 \cos(\theta - \theta_{0ff}), -90° + \theta_{0ff} \leq \theta \leq 90° - \theta_{0ff} \quad (1)$$

$$P_R = P_0 \cos(\theta + \theta_{0ff}), -90° + \theta_{0ff} \leq \theta \leq 90° - \theta_{0ff} \quad (2)$$

By taking the difference over sum ratio, it is possible to eliminate the unknown pressure amplitude P_0 giving

$$\frac{P_L - P_R}{P_L + P_R} = \frac{P_0 \cos(\theta - \theta_{0ff}) - P_0 \cos(\theta + \theta_{0ff})}{P_0 \cos(\theta - \theta_{0ff}) + P_0 \cos(\theta + \theta_{0ff})}$$

$$= \tan(\theta)\tan(\theta_{0ff}) \quad (3)$$

The angle, θ can be obtained as

$$\theta = tan^{-1}\left(\frac{1}{\tan(\theta_{0ff})}\frac{P_L - P_R}{P_L + P_R}\right), -90° + \theta_{0ff} \leq \theta \leq 90° - \theta_{0ff} \quad (4)$$

Figure 4 shows simulated (normalized) responses of two sensors when the θ_{off} is 30°. The two responses are shifted by 60° as expected based on Equations (1) and (2).

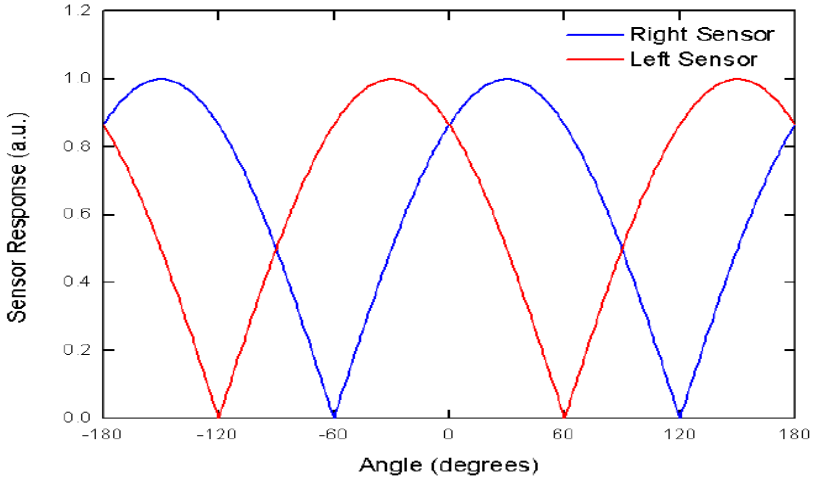

Figure 4. The simulated responses of two sensors canted at 30º.
Source: [22].

Figure 5 is obtained by taking the difference over sum of the signal in Figure 4 which shows the tangent dependent expected from Equation 3 within ±60° range of incident angles.

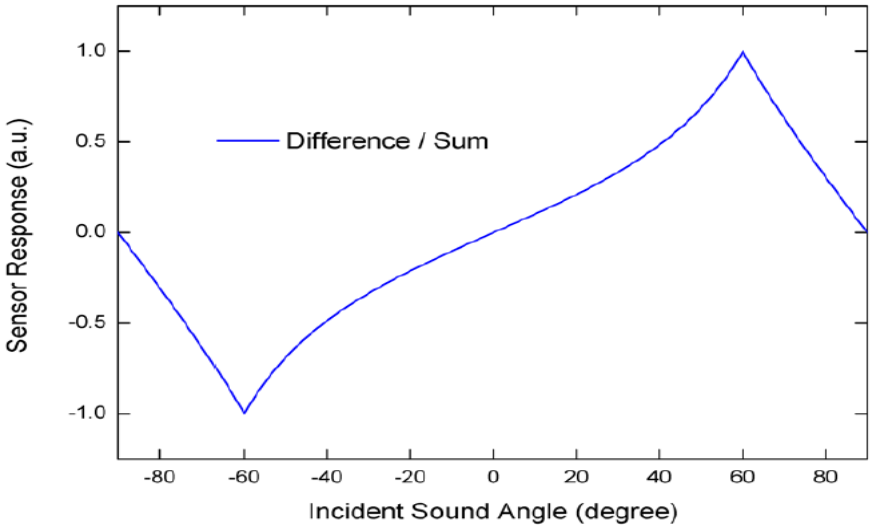

Figure 5. The difference over sum of the canted sensor assembly based on the data in Figure 4. Source: [22].

The goal of this work is to extend the canted sensor approach developed to find sound direction in air and underwater applications.

B. OBJECTIVE AND THESIS STRUCTURE

The purpose of the thesis is to find the exact direction of a sound using two canted MEMS sensors underwater. This is an extended version of the study using single sensor with boot underwater.

This thesis is composed of 5 chapters. Chapter I provides the theory of finding the basic principles of MEMS sensors through the parasite fly, *Ormia Ochracea* and the direction of sound using two divided sensors.

Chapter II explains the character of the sensors, boot design and how sensors were designed in experiments conducted in the thesis.

Chapter III describes how two sensors are tested in the anechoic chamber. It means these sensors are checked to find the direction of a sound in air per different angle offset between them, before taking experiments underwater. The results are then compared with the result of experiments with a single MEMS sensor in air.

Chapter IV presents sensors tested underwater per different offset angle between the two sensors. These tests were performed to check how accurately two sensors track the sound source. In addition, the utility of this experiment is verified by comparing the resulting values using the single sensor.

Chapter V presents the conclusions of this thesis and future improvements.

II. CANTED SENSORS DESIGN FOR UNDERWATER OPERATION

The bearing of sound can be determined using many different approaches [23–28]. These include hydrophone arrays, accelerometers, hotwire sensors and neutral buoyant sensors. The SRL at NPS is developing MEMS-based underwater directional sensors [21]. It was found that a single underwater MEMS sensor is unable to resolve the right-left ambiguity due to its cosine directivity pattern. However, a previous study has confirmed that two canted MEMS directional sound sensors operated in air are able to find direction of sound unambiguously [21, 23, 29].

In this chapter, an approach to package two MEMS sensors at a canted angle to operate underwater will be described. Several important considerations have been taken into account in the design of the sensor housing and mount for mounting the sensors at a canted angle. The sensors need to be housed in a non-conducting fluid that has acoustic impedance close to that of the water. A rubber boot with good acoustic transmission was constructed for housing the sensor.

A. SENSOR HOUSING

1. Material

In a previous work [21], several different materials were considered to construct the boot that protects the sensor from water while allowing good sound transmission within the frequency range of interest (50-600 Hz). It was found that PMC-780 polyurethane meets most of these requirements. The measurements, which were carried out using three different boot thicknesses, found that PMC-780 in the 50–600 Hz frequency range is the best. The signal from a sound source measured using a hydrophone was not affected by the presence of a boot surrounding it as shown Figure 6 [21]. The study was performed using a set of 5-mm thickness boots.

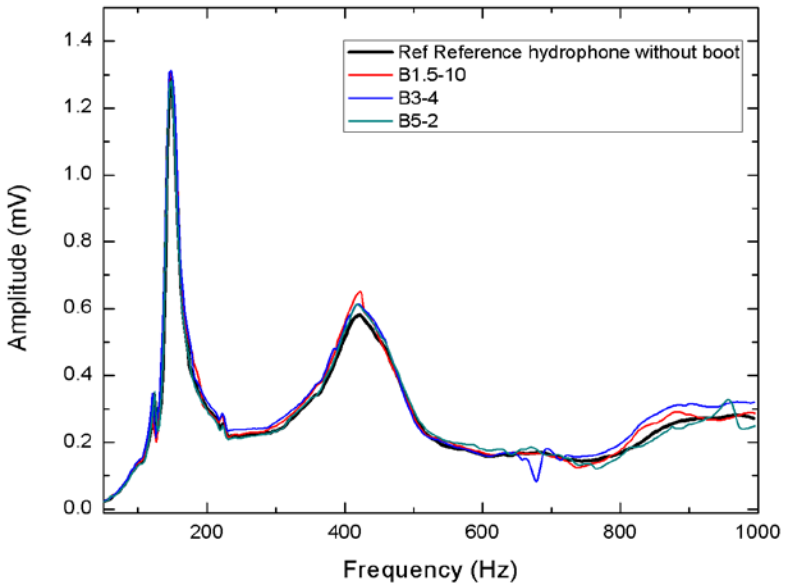

Figure 6. Comparison of acoustic transmissions for each material by thickness. Source: [21].

However, a recent study by Roberts [23] found that when the thickness of the boot is reduced to 3mm thickness the boot made of PMC-780 affected the sensitivity of the MEMS sensor. The 3mm and 5mm thickness boots affected different part of the acoustic frequency range which was suspected to be due to resonances of the boots which affected the sound transmission. [23]. To understand this behavior a set of 3 mm and 5 mm thickness boots were fabricated as outlined below.

2. Construction of the Boots

The mold for fabricating 5mm thickness boots of the sensor housing was originally designed by Espinoza Peyrot [21] and was redesigned by Roberts [23] with 3mm thickness, as shown in Figure 7. The details of boot fabrication steps are described in the Appendix.

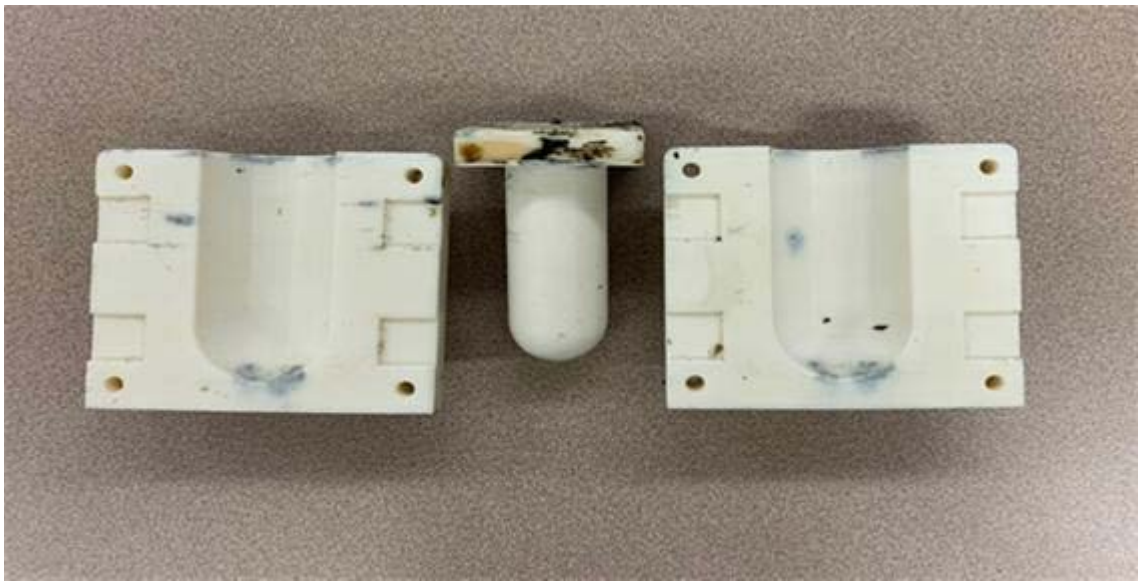

Figure 7. Mold used for fabricating boots for sensor housing

A fabricated boot along with the components used for sensor assembly (O-ring, metal coupling to boot, flange, chain clamp, and HDMI connector) is shown in Figure 8. The boot is filled with PSF-1cSt silicone oil which is non-conducting and has acoustic impedance similar to that of water. The sensors are immersed in it during the operation.

Figure 8. Components used for assembling sensor housing

B. ACOUSTIC TRANSMISSION OF BOOT

Experiments were conducted using a hydrophone to determine the effect of boot thickness on acoustic transmission through it. The UW30 underwater speaker was used as the sound source in this experiment. A B&K 8103 hydrophone was chosen as the sensor since it has a flat response in the frequency range of interest. First, the characteristics of the sound source were measured using the bare hydrophone. Then, the hydrophone signal was recorded when it was immersed in boots with 3 mm and 5 mm thickness filled with silicone oil. The schematics of the experimental setup are shown in Figure 9. The measured hydrophone signals without and with the boot attached to it are shown in Figure 10. Figure 11 shows the transmission characteristics of the boot by dividing the signals with boot by without boot. It can be seen in Figure 11 that the boot transmission characteristics varies with it thickness. The hydrophone with the 5 mm thickness boot detected a relatively flat response at the resonance frequency of the MEMS sensor (~ 510 Hz) while the 3-mm thickness boot shows resonance characteristics in the 500–600 Hz frequency range. This may be due to the resonance mode of the boot itself. Thus, 5 mm thickness boots were employed for characterization of the MEMS sensors.

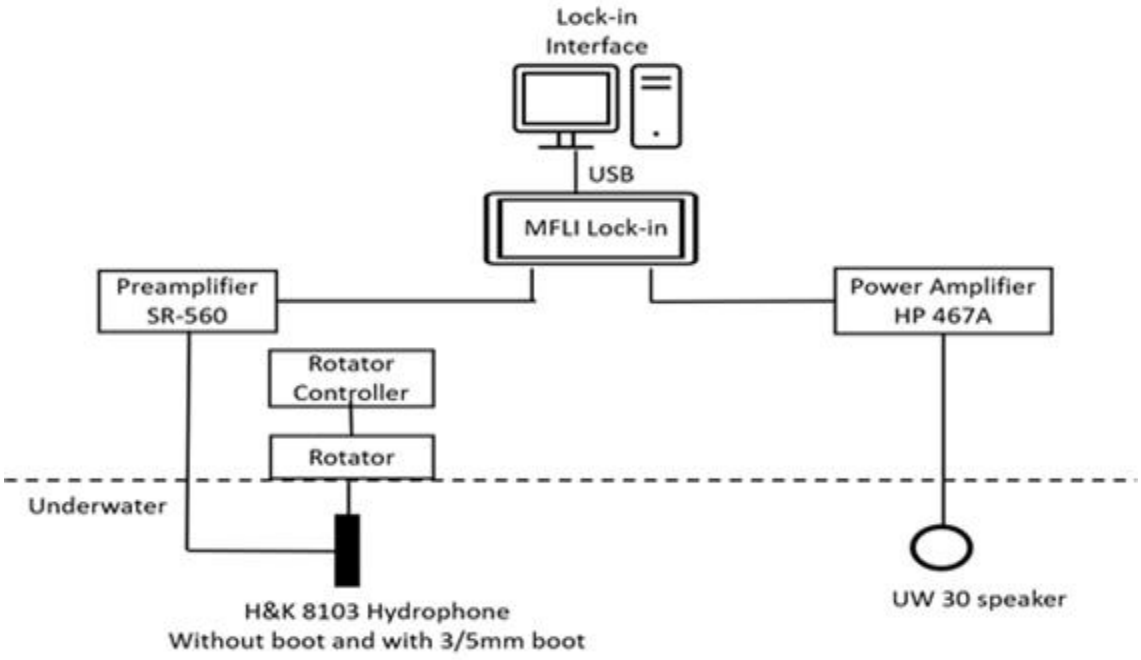

Figure 9. Schematic of experiment setup

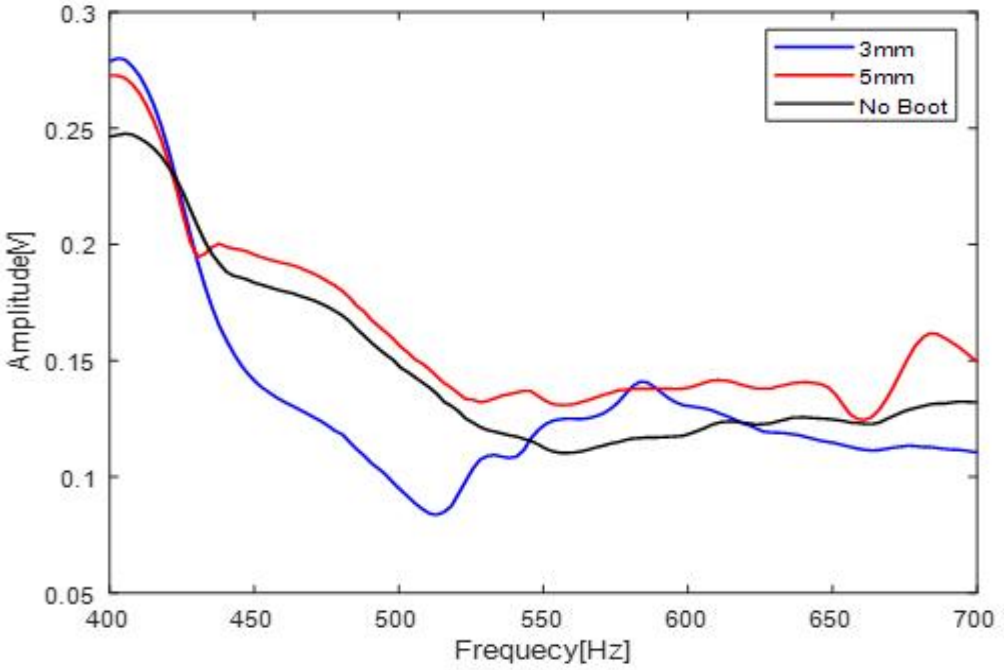

Figure 10. Hydrophone response without boot and with 3/5mm thickness boot underwater

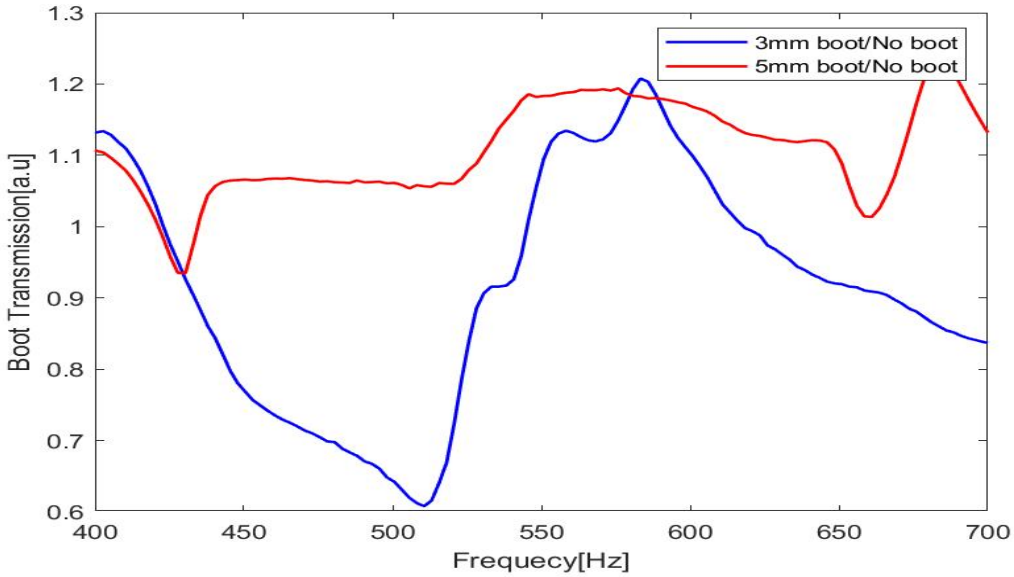

Figure 11. Hydrophone response with 3- and 5-mm thickness boots divided by hydrophone response without boot

C. INTEGRATION OF SENSOR AND HOUSING

The circuit board containing the sensor and readout electronics was connected to the flange via a sealed HDMI connector as shown in Figure 12 (a). Marine sealant was used to secure the circuit board to the flange as described in detail by Roberts [23]. Then the boot was filled with silicone oil, the sensor was immersed in it and sealed using an O-ring and chain clamp as shown in Figure 12 (b). Two identical sensors were prepared using this procedure to be integrated with the fixture used for mounting them at a canted angle. The design and fabrication of the fixture will be presented next.

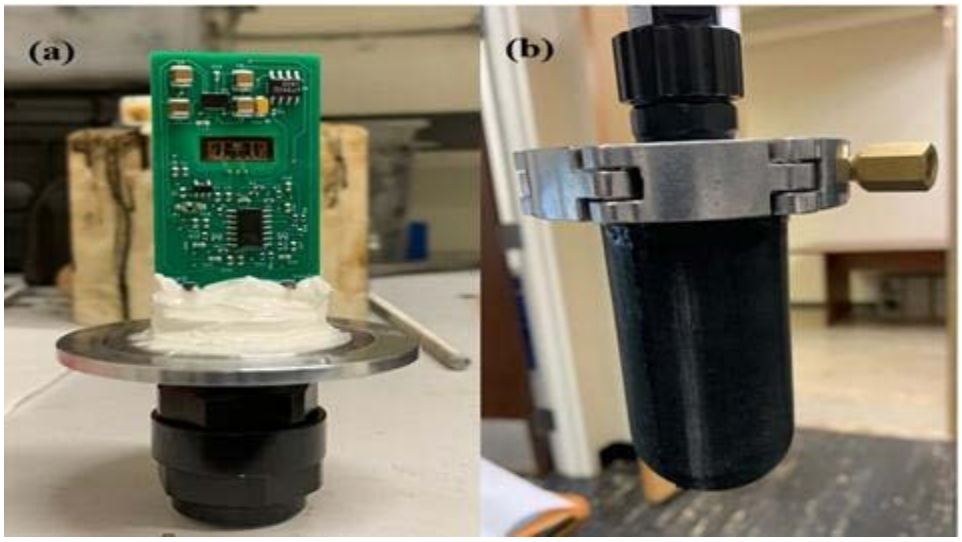

Figure 12. Sensor and circuit board integrated with the flange (a) and the sensor assembly integrated with the boot (b)

D. FIXTURE FOR MOUNTING CANTED SENSORS

As described earlier, two sensors needed to be mounted at a canted angle to prevent the left and right ambiguity on bearing of sound. The previous studies were carried out using a single sound sensor found to have a cosine directivity pattern [22]. A mount was designed using Solidworks CAD software such that two packaged sensors (see Figure 12 [b]) can be mounted at an offset angle, θ_{off} as illustrated in Figures 13(a) and (b) for 15^{o} and 30^{o} angles, respectively. A set of holes in the middle were made at

intersection points of the planes of the sensors at different offset angles and taken to be the rotation axis.

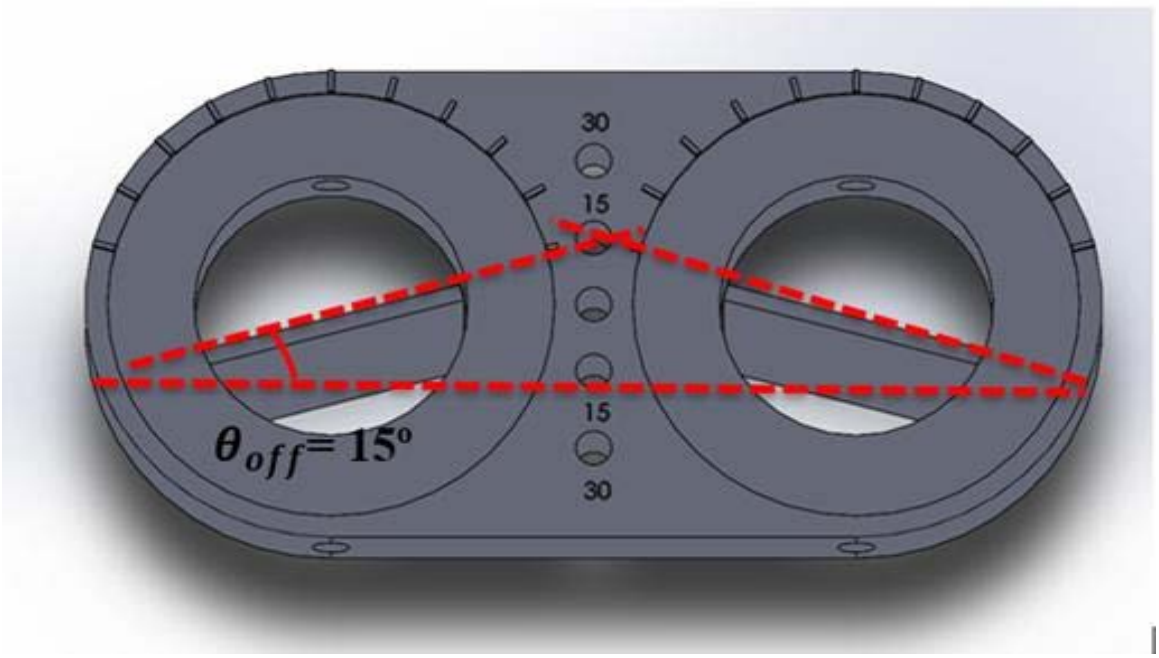

(a)

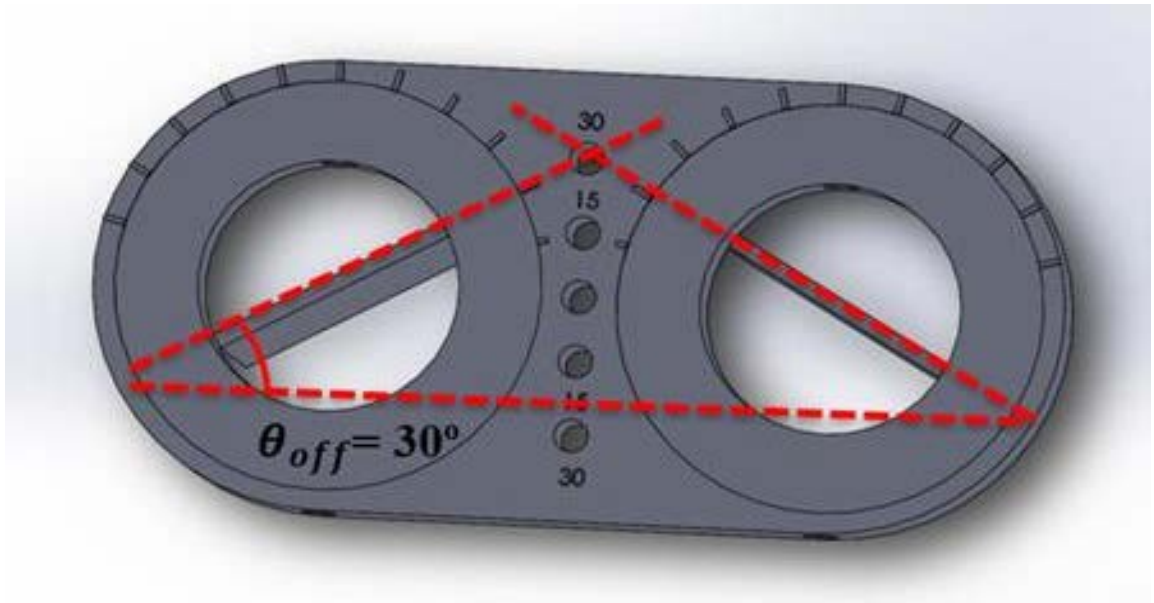

(b)

Figure 13. The concept of mounting of two canted sensors at (a) $\theta_{off} = 15°$ and (b) $\theta_{off} = 30°$

The fixture was fabricated using a 3D printer and the sensors packaged in their respective boots were secured using four bolts inserted through tapped holes on the sides (see Figure 14).

Figure 14. The 3D printed fixture for mounting the sensors.

III. MEASUREMENTS IN ANECHOIC CHAMBER

Initial measurement of the MEMS sensors was carried out in the NPS anechoic chamber to probe their functionality in air. Two nearly identical sensors arranged at a canted angle using the fixture shown in Figure 14 were mounted on the rotating table to determine their directional responses. In addition, these measurements helpedus to optimize the canting angle between the two sensors before carrying out the underwater response. First, directional response of two canted sensors without the boot was measured at different canted angles. Then, the same measurements were repeated with sensors mounted in boots filled with silicone oil. The MEMS sensors utilized in the measurement, experimental setup employed, and results of the tests are presented in this chapter.

A. SENSORS DESIGN

The MEMS acoustic sensors used in the measurements were designed by our group using COMSOL finite element modeling. The sensor was based on a two-wing design as described in Collins [30]. It was designed to have a desired resonance frequency by controlling the dimensions. Figure 15 shows an optical micrograph of one of the MEMS sensors used in the measurements. The individual sensor characteristics both in air and underwater were carried out by Roberts [23] showing the resonance characteristics and expected cosine directional response.

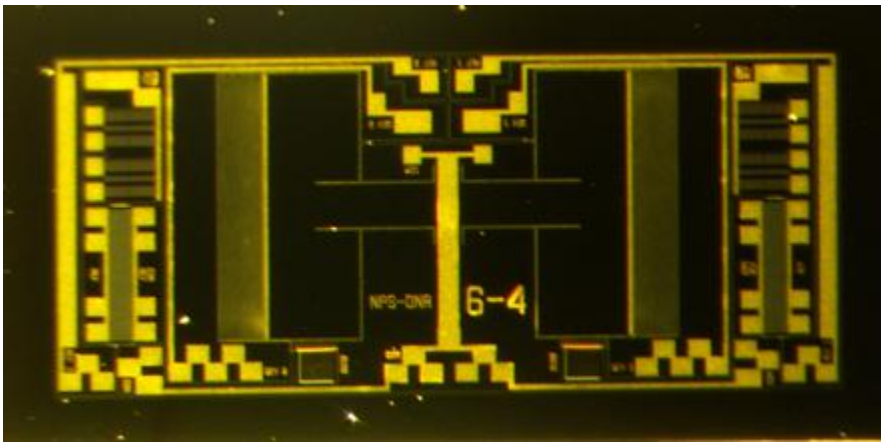

Figure 15. Optical Micrograph of Underwater MEMS Sensor

B. EXPERIMENTAL SETUP

Before performing measurements using the water tank, it was necessary to probe the characteristics of MEMS sensors in air to make sure they were functioning as expected. The experiments were carried out by arranging two nearly identical MEMS sensors mounted at a canted angle in the NPS anechoic chamber, as depicted in Figure 16.

A JBL 2380A speaker with a horn was used as the sound source. The responses from the two sensors were recorded using two MFLI lock-in amplifiers as schematically shown in Figure 16. The speaker was connected to the master lock-in amplifier via an audio amplifier. The two lock-in amplifiers were synchronized as master and slave mode to measure the outputs of the two sensors simultaneously. The canted sensor mount with two MEMS sensors was attached to the rotator in the anechoic chamber which can be controlled by the rotator controller in the control room.

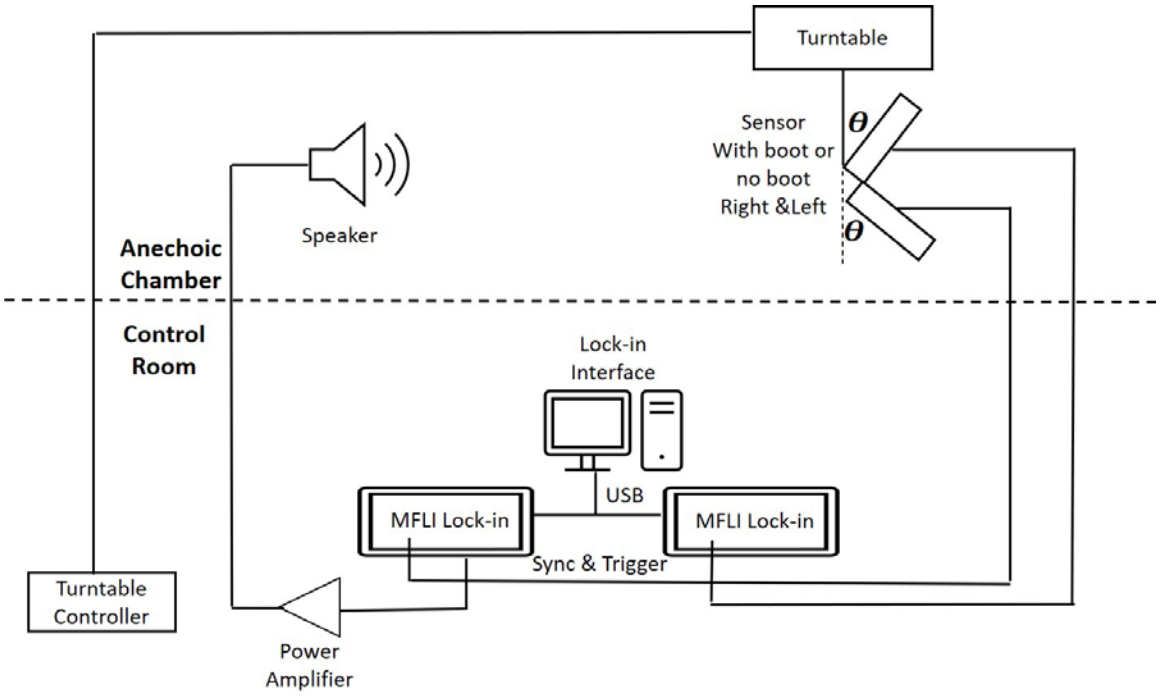

Figure 16. Schematic of Experimental setup in the anechoic chamber

The measurements were divided into two parts. First was to perform measurements using only two canted sensors without the boots attached to them as shown in Figure 17 (a). The resonance frequency of the two sensors was measured by sweeping the frequency. The rotational measurements were then performed at the resonance frequency (2690Hz) for two offset angles (15º and 30º) between two sensors. Next, the same set of measurements were carried out using two MEMS sensors immersed in boots filled with silicone oil. For measuring the sound pressure inside the boot, a reference hydrophone (B&K 8103) was mounted in a similar boot filled with silicone oil. The signal from the hydrophone was amplified using an SR 650 preamplifier connected to a lock-in amplifier. The gain of the preamplifier was set to 100. By sweeping frequency, the resonance frequency of the sensors was found. A relatively long pole was attached to the rotator to reduce the tension of HDMI cables used for connecting the sensors to the lock-in amplifiers sitting outside of the anechoic chamber, as shown in Figure 17 (b). As in the earlier measurements, responses of the sensors with canted angles 15º and 30º were measured.

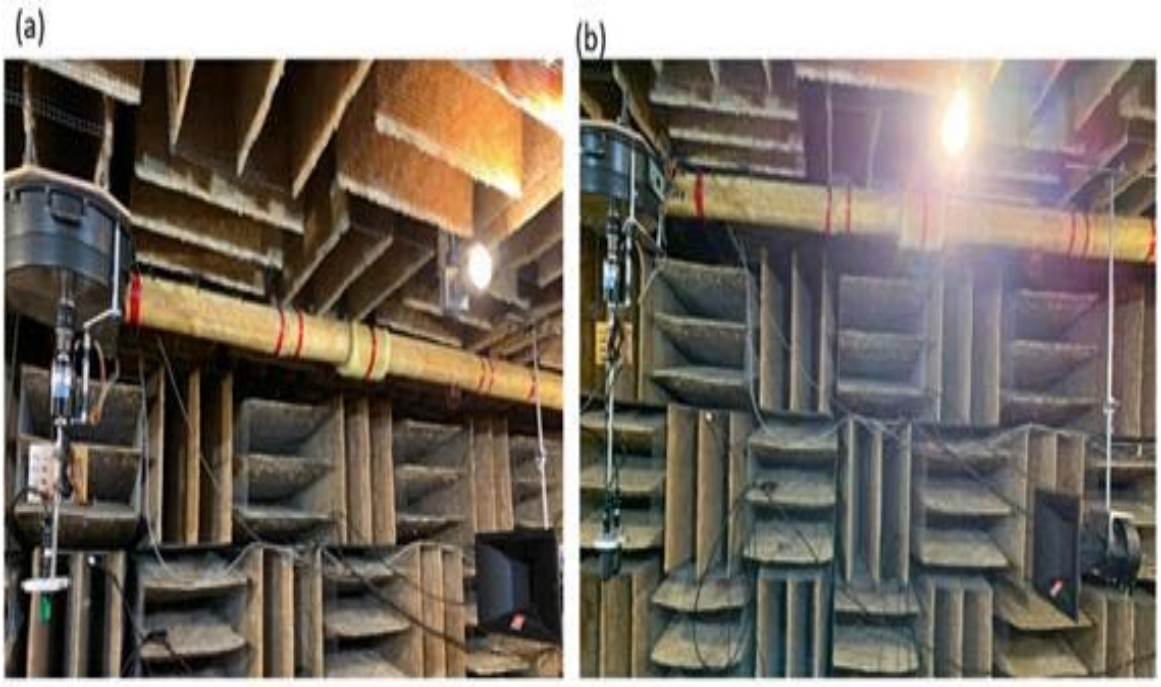

Figure 17. Canted MEMS sensors assembly mounted to the rotating table in the anechoic chamber without the boot attached (a) and with boot attached (b)

C. RESULT AND ANALYSIS

1. Measurements without Boot

The frequency response measurement was carried out by sweeping frequency from 300 Hz to 3000 Hz in 2.5 Hz steps. It was found that the resonance frequencies of the two sensors were 2687 Hz and 2692 Hz. Figure 18 shows the measured directional responses of the two sensors with a 15^{o} canted angle. The data presented in Figure 18 were normalized by dividing them using their respective peak values.

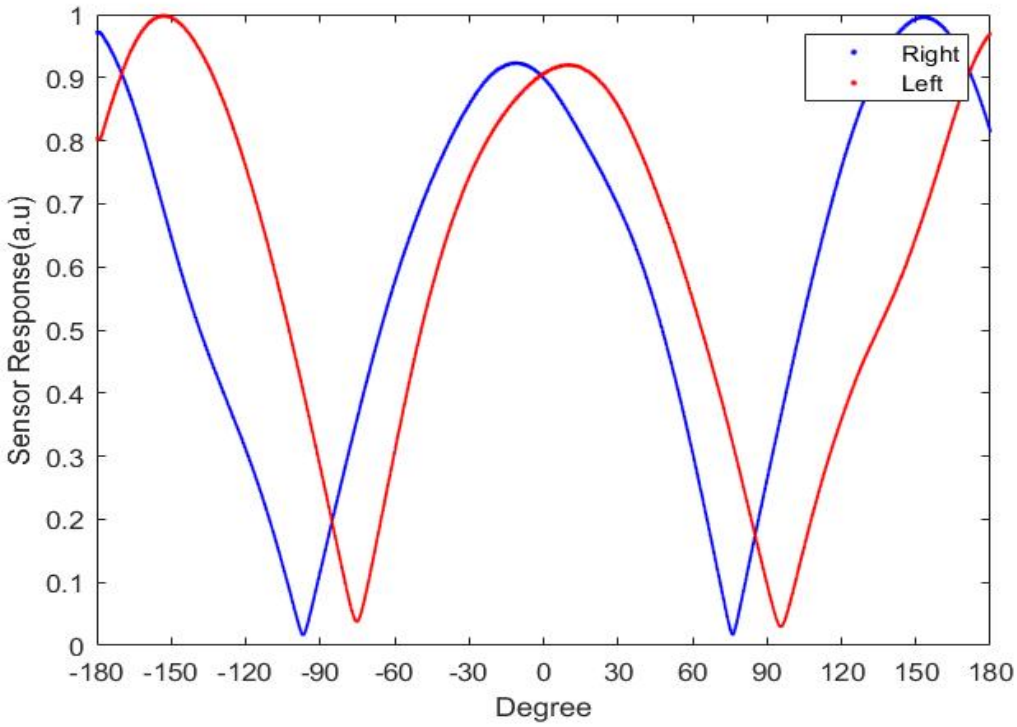

Figure 18. The normalized responses of two sensors canted at 15^{o} without boot

Figure 19 shows the difference over sum of the two responses shown in Figure 18. It can be seen that the difference over sum provides a way to determine direction of incident sound unambiguously as described in Chapter II. The set of measurements were repeated for 30^{o} canted angle and the results are shown in figures 20 and 21. As expected, at 30^{o} canted angle the unambiguous detection range is smaller as predicted by the analysis in Chapter II.

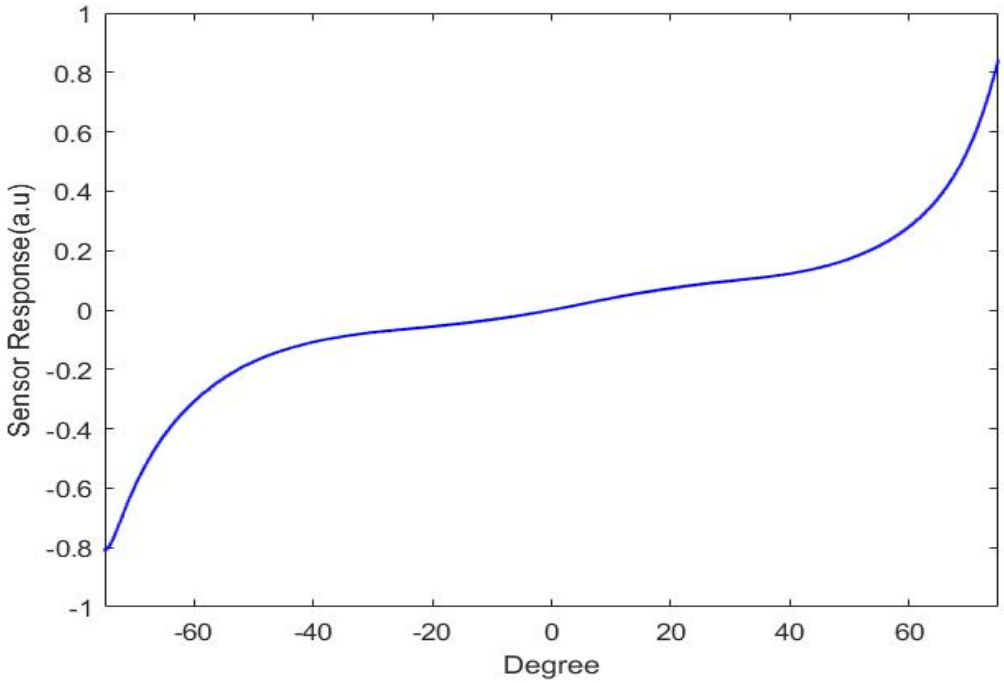

Figure 19. The difference over sum of the responses using the data in Figure 18

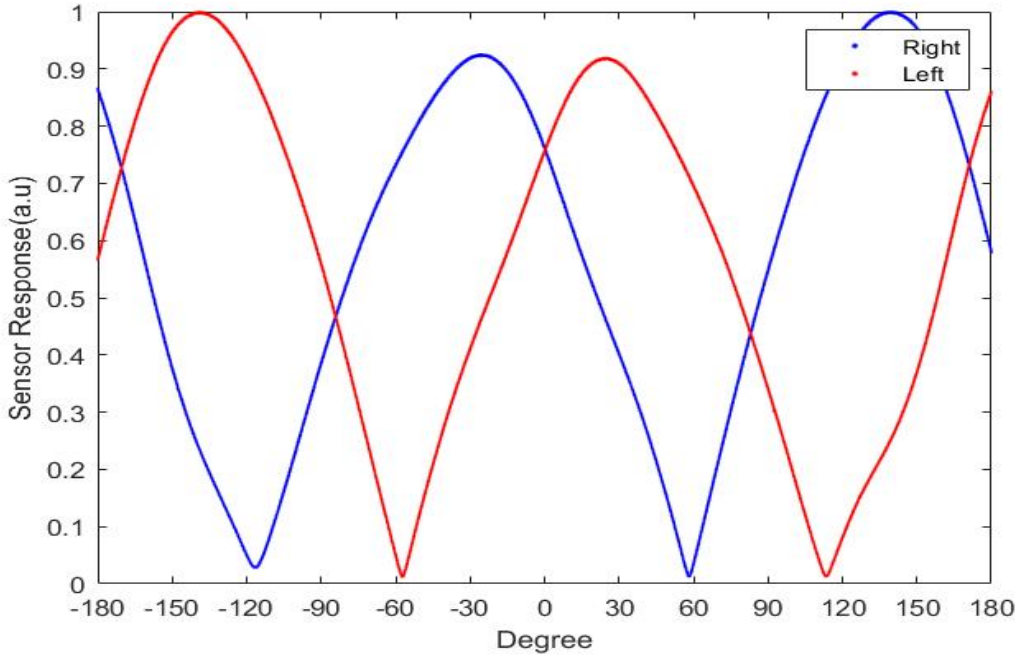

Figure 20. The normalized responses of two sensors canted at 30^{o} without boot

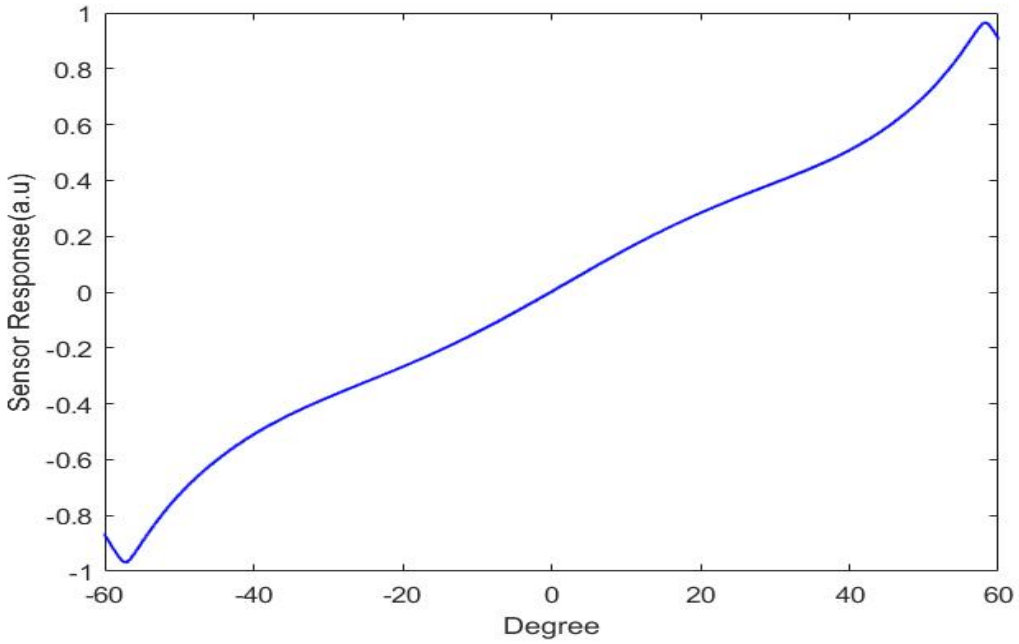

Figure 21. The difference over sum of the responses using the data in Figure 20

2. Measurements with Boot

As in the case of the experiments, the frequency responses of the sensors were carried out from 300 Hz to 1150 Hz with 2.5 Hz steps. The lower frequency range is caused by the operation of the MEMS sensors in silicone oil affected by the mass loading [10]. A reference hydrophone mounted in a boot filled with oil was used to determine the acoustic pressure inside the boot. The data from the reference hydrophone was used to obtain sensitivity of MEMS sensors as follows.

Sensitivity is defined as measured signal voltage (V) to incident sound pressure (P). The sensitivity of the hydrophone (M) used in the measurement is about 23 V/μPa. During this experiment, the hydrophone was connected to the SR 560 preamplifier with gain (G) of 100. The measured hydrophone signal V_{ref} and its sensitivity are used to estimate the sound pressure using

$$P = \frac{V_{ref}}{GM}. \tag{10}$$

Then, the sensitivity of the MEMS sensor M_s can be obtained by using the measured signal, V_{signal} as

$$M_s = \frac{G\,M\,V_{signal}}{V_{ref}}. \tag{11}$$

Measured sensitivities of the two MEMS sensors are shown in Figure 22. The expected resonance frequency of the sensors is around 500 Hz which somewhat masked by the vibrations of the circuit board integrated with the sensor. The sensors used had same characteristics on specification, but they had slightly different sensitivity.

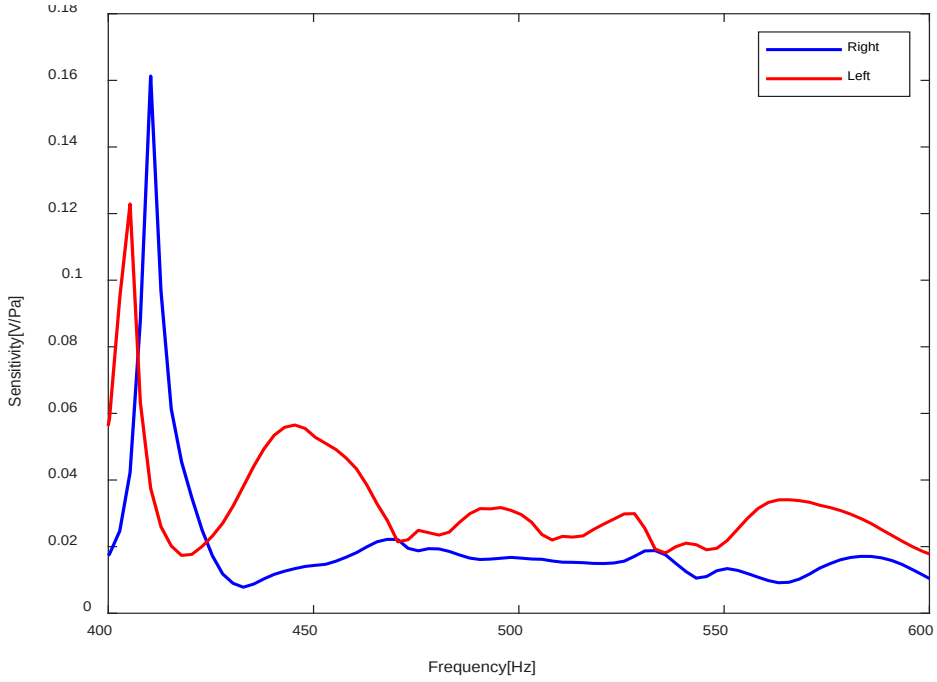

Figure 22. Sensitivity of the two sensors with frequency

Following the same steps as in the measurement without the boot, directional responses were measured for canted angles 15° and 30°. Then, the difference over sum for each angle was calculated. Figures 23 and 24 show the directional responses for the two sensors and difference over sum, respectively, at 15° canted angle. As predicted, it

can be seen in Figure 24 that from approximately -75° to +75° the direction can be uniquely obtained using the canted sensor assembly.

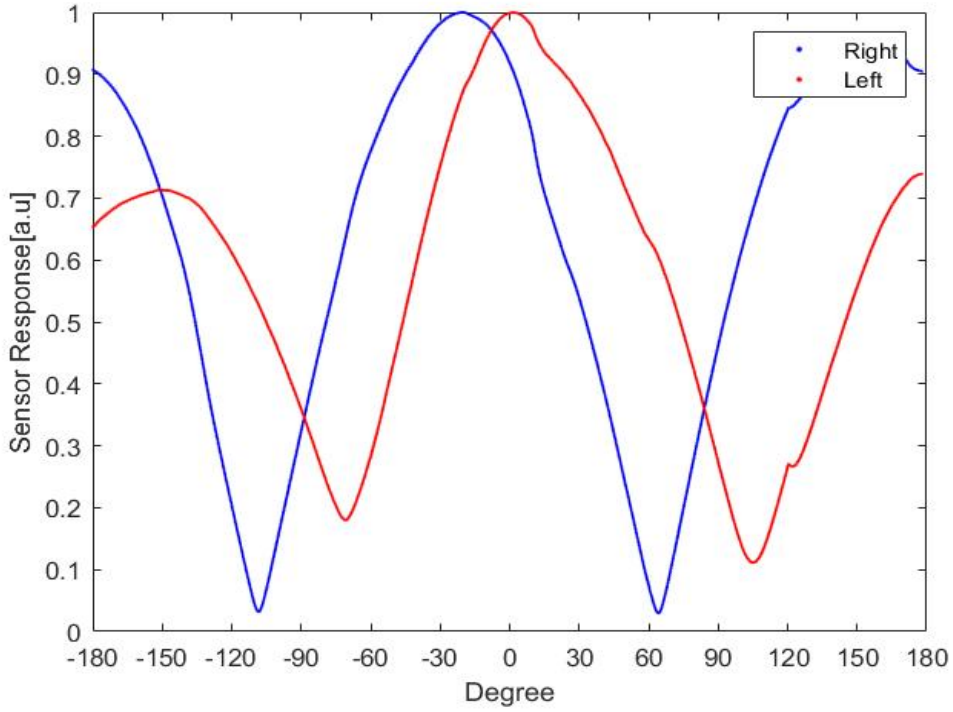

Figure 23. The normalized responses of two sensors canted at 15^{o} without boot.

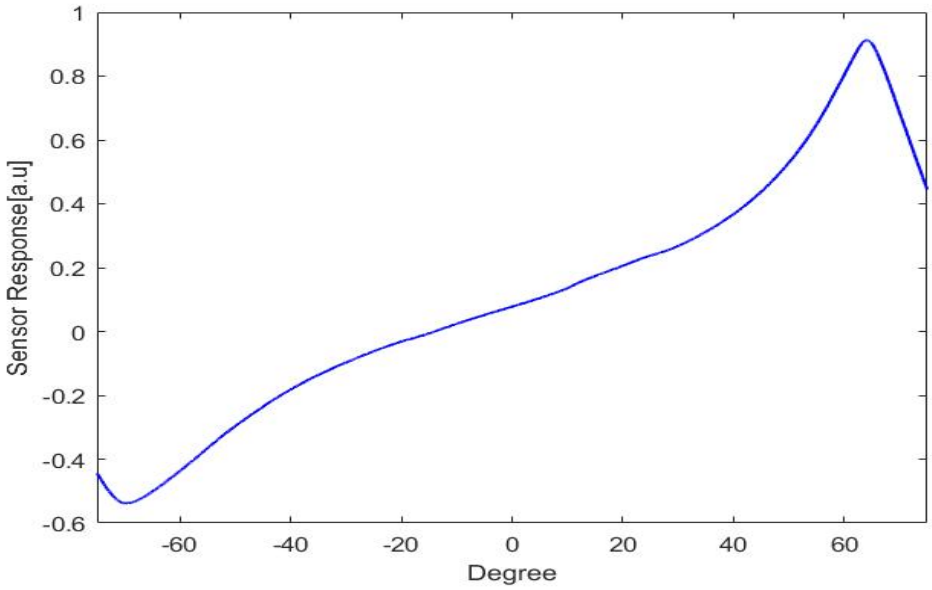

Figure 24. The difference over sum of the responses using the data in Figure 23.

Figure 25 and 26 show the directional responses for the two sensors and difference over sum, respectively at 30° canted angle. In this case, as seen in Figure 26 the unambiguous detection range narrowed to approximately -60° to +60° due to the larger canted angle employed. However, a grater difference over sum range was obtained as predicted by Equation 3.

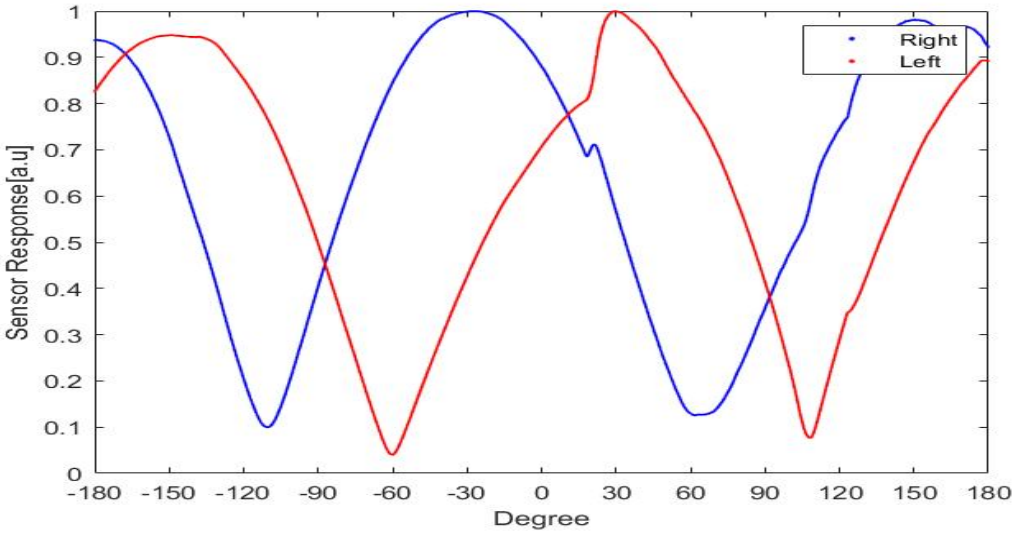

Figure 25. The normalized responses of two sensors canted at 30^{o} with boot

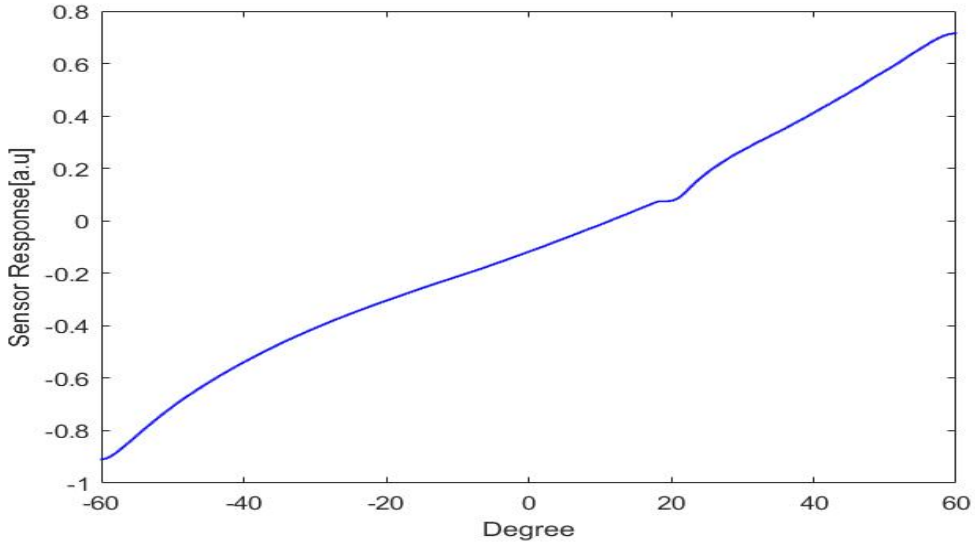

Figure 26. The difference over sum of the responses using the data in Figure 25

THIS PAGE INTENTIONALLY LEFT BLANK

IV. OPERATION OF CANTED SENSORS UNDERWATER

In Chapter III, it was found that two underwater MEMS sensors mounted at a canted angle could find the direction of sound when operated in air. Before experimenting with the two canted sensors underwater, each individual sensor's performance was characterized by measuring its frequency and directional responses. Then, the directional response of two canted sensors mounted on the fixture was carried out. In this chapter, measurements of the canted sensors underwater carried out in the NPS water tank will be presented.

A. EXPERIMENTAL SETUP

The UW30 underwater speaker was used as the sound source in the experiment. It was located about 1 meter below the water surface of the water tank. The internal oscillator output of MFLI lock-in amplifier fed through the HP 467A power amplifier was used as input to the speaker as schematically illustrated in Figure 27. The sensor was fixed to a rod which is inserted into HA5C rotator and adjusted to the same height as the speaker. The HDMI cable connected to the sensor and was loosely tied to the rod to reduce the cable tension. The rotator was placed on thick foam slabs and concrete blocks to reduce coupling of mechanical vibrations from the speaker. The rotator was operated by its controller to set either the desired angle or continuous rotation. The distance between the sensor and the speaker was about 0.5 m. The speaker was connected to the master lock-in amplifier. The two sensors were powered by an HP Dual power supply model E3620A. The sensors' outputs were each measured by a lock-in amplifier. The amplifiers were both connected to the computer via USB, through which data was transferred to the computer and they were controlled by the Lab-on program installed. The two lock-in amplifiers were synchronized with master and slave configuration to simultaneously measure outputs of the sensors. A reference hydrophone B&K 8103 packaged in a housing similar to that of the sensors was used to measure sound pressure. During the sound pressure measurement, the sensors were replaced by the hydrophone.

The signal from the hydrophone was amplified using the SR560 preamplifier with a gain of 100. Figure 27 shows a picture of the experimental setup.

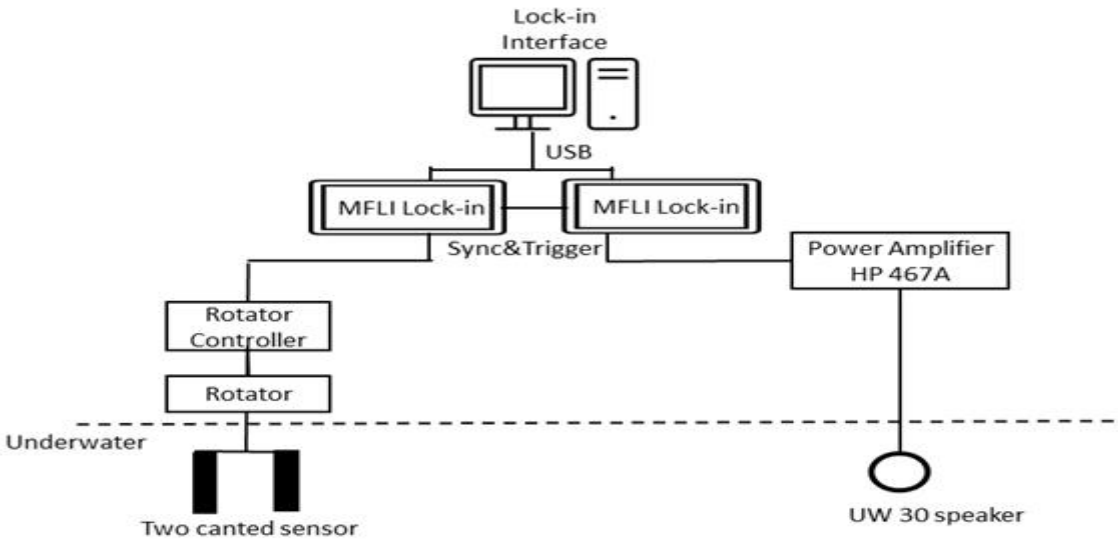

Figure 27. Schematics of experimental setup for water tank measurement

Rod (a), speaker (b), rotator (c), rotator controller (d), MFLI lock-in amplifier (e), and power amplifier (f).

Figure 28. Picture of experimental setup in the water tank

B. RESULT AND ANALYSIS

1. Response of Single Sensor

In the experiment, the frequency response of each sensor was carried out from 0° to 360° in 10° steps. The output signal of each sensor was measured from 300 Hz to 700 Hz with 2.5 Hz steps. The frequency response of the reference hydrophone housed in a boot similar to that of the sensor was carried out within the same frequency span to determine the sound pressure in the boot. Figure 29 shows the sensitivity (V/Pa) as a function of frequency for the two sensors, parametrized by the sound direction of arrival. The responses in Figure 29 show a relatively narrow peak around 430 Hz and a broad peak centered around 520 Hz. The peak at 430 Hz is most likely due to resonant mode of the circuit board where the sensor is attached. The broader peak around 520 Hz is from the bending resonance mode of the sensor. The peak position is close to the simulated data reported previously by Roberts [12]. It can be seen in Figure 29 that the sensitivity gets smaller as the direction of arrival of sound changes from 0° to 90°. The responses of the two sensors were found to be slightly different most likely due to packaging. The responses found to have similar directional characteristics at broader peak centered around 520 Hz.

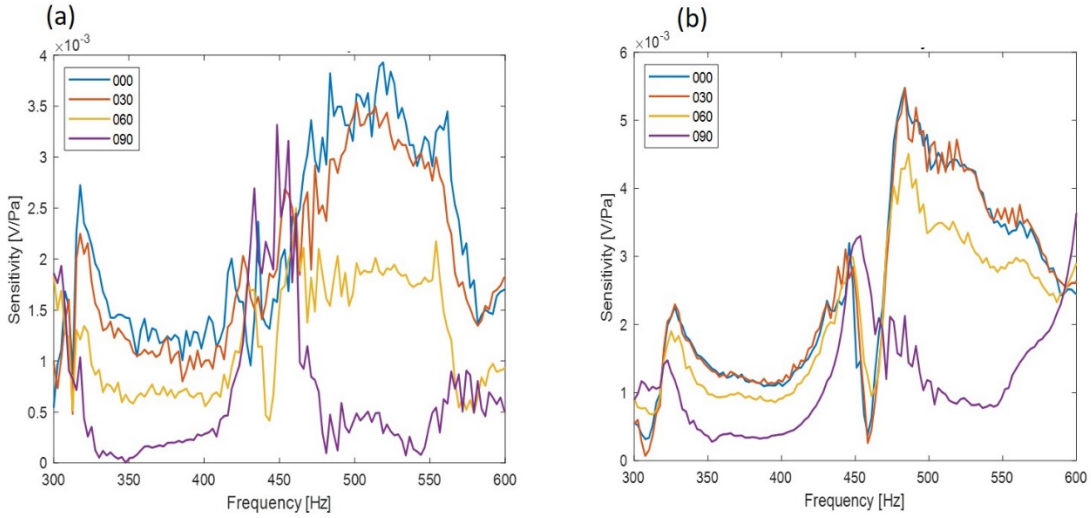

The numbers on legend are the degree to face to the sound source. Sensitivity was gotten per 30° to find the resonance frequency of sensors.

Figure 29. Measured sensitivity of right (a) and left (b) sensors

In addition to the frequency response at different incident angles of incident of sound, the directional response was also measured at the resonance frequency of the sensor. Figure 30 shows the measured directional responses of the two sensors at 520 Hz. The measurements show the expected cosine dependence to the incident direction and agrees well with the measurements carried out in the anechoic chamber despite the differences in frequency responses. Figure 31 shows the directivity patterns of the two sensors in polar coordinates. The slight difference in directivity patterns for the two sensors is most likely due to misalignments during the packaging of the sensor assembly as well as asymmetries associated with mounting hardware.

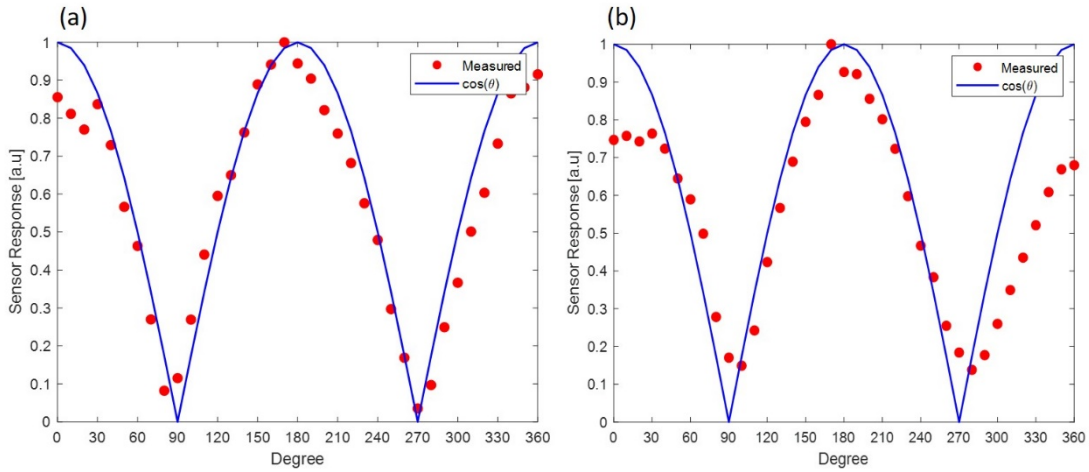

Figure 30. The directionality of right (a) and left (b) sensor in Cartesian coordinates

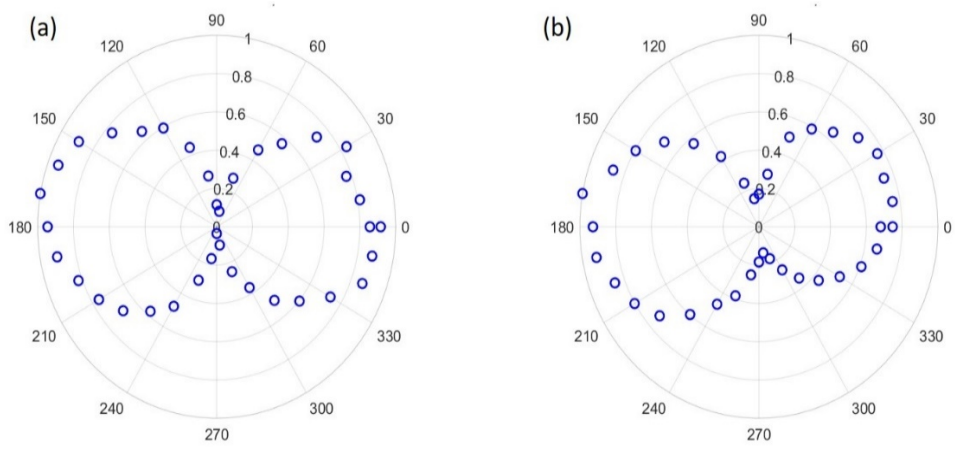

Figure 31. The directionality of right (a) and left (b) sensor using polar coordinates

2. Response of Two Canted Sensors

The directional response of the canted sensors was measured using the same fixture used during the measurements carried out in the anechoic chamber. Figure 32 shows the directional response of the two sensors canted at 15°. The data shows that each sensor response follows cosine-like behavior with some deviation which is mainly due to effects of mounting hardware on the sound field as well as relatively large separation of the two sensors. As expected, the two responses are shifted from one another due to the canted angles. The measured difference between two responses of the sensors is 20°, which is smaller than the theoretically expected 30°. Note that the theoretical analysis assumed that there is no interaction between the sensors acoustically and realistic experiments, taking into account of the circuit board, produced a smaller shift similar to the one observed in the experimental results here presented [21].

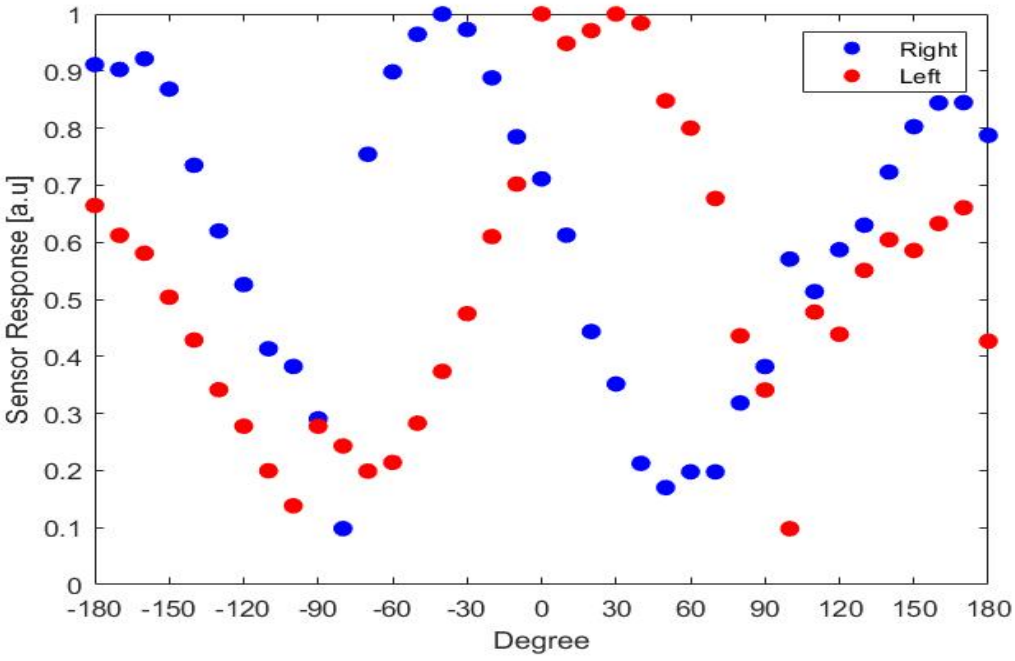

Figure 32. Normalized responses of two sensors canted at 15° with boot underwater.

Figure 33 shows the difference over sum using the data in Figure 32. It can be seen in Figure 33 that the difference over sum shows a unique value at each angle of incident in a broad range allowing the determination of direction of sound unambiguously.

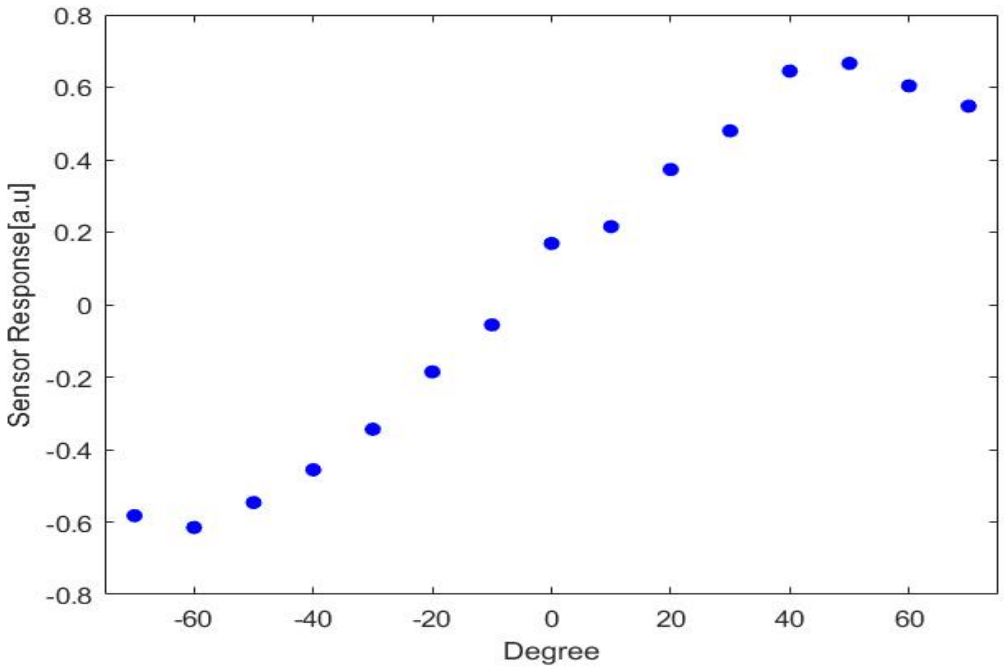

Figure 33. The difference over sum of the canted sensor assembly using the data in Figure 32.

V. CONCLUSION

A. SUMMARY

The main goal of this thesis was to operate two underwater MEMS sensors in canted configuration to uniquely determine the bearing of sound sources. Each MEMS sensor has a cosine directivity pattern which results in right-left ambiguity. To solve this problem, experiments were conducted underwater using two canted MEMS sensors. The two signals from the sensors were processed by taking difference over sum to determine the bearing of sound.

The two MEMS sensors employed in the measurements have bending resonance frequencies around 2500 Hz when operated in air. A custom fixture was fabricated to place the two sensors at a canted angle. Initial measurements were carried out in air to make sure that the fixture fabricated to mount the sensors at a canted angle performs as expected. The result showed that, using two sensors in air, the direction of sound can be uniquely determined over a prescribed range of bearing depending on the canted angle employed. The next set of experiments were also carried out in air with the MEMS sensors packaged in a sound transparent housing suitable for underwater operation. Obviously, the sound transmission through the housing is not optimal for measurements in air. However, measurements showed that canted sensor assembly functioned as expected. The bending resonance frequency of the sensor was found to be around 510 Hz due to its operation in silicone oil used in the underwater housing. The reduction of resonance frequency is primarily due to mass loading from the silicone oil. It was found that the 15° canted configuration provided the broad angular range for unambiguous determination of bearing of sound with relatively good sensitivity. In addition, with a 30°canted angle the angular range narrowed while providing slightly higher sensitivity.

The final set of experiments were carried out in NPS underwater tank to assess the performance of the canted sensor assembly in an underwater environment. Initially, the frequency responses of the sensors were measured to find the bending resonance frequency which, as expected, closely matched with that observed in the anechoic

chamber. Then, the directional response of the canted assembly was measured at a canted angle of 15°. The results showed nearly cosine directional responses from the two sensors. The difference over sum metric used for extracting the direction showed the expected tan theta dependence. The measurements carried out in this thesis showed the canted MEMs sensor could be used for determining bearing of underwater sound sources unambiguously.

B. RECOMMENDATIONS

It was found during the measurements underwater that the boot and circuit board resonances affected the response of the sensor. The 5 mm thickness boot was able to reduce its effect on the frequency response compared to the 3 mm thickness boot. It is important in future studies to focus on finding optimum boot thickness to minimize interference on the sensor response.

The circuit board that was integrated with the sensor is mounted to the flange of the sensor housing which itself acted as a cantilever with its own resonance frequencies. In addition, it also responded mechanically similar to the sensor with directional dependence oscillations affecting the sensor response. The mounting of the circuit board should be strengthened to minimize its vibrations.

Finally, it is necessary that the experiments be conducted using a bigger water tank such as in Transducer Evaluation Center (TRANSDEC) in San Diego to minimize the reflected sound waves that affect the directional response of the sensor.

APPENDIX. 5MM THICKNESS BOOT CONSTRUCTION

1) The ratio between part A and B of PMC-780 is part A 60g and B 30g

2) Add 4 drops of strong black coloring agent to part B and stir well

3) Put both part A and B inside vacuum chamber and set the pressure to 28’’Hg

4) Apply vacuum once for 15 minutes to remove surface bubbles

5) Prepare the mold while part A and B are in vacuum. Screw 4 on sides, 4 up right. Tighten them one by one.

6) Take the two containers from the vacuum chamber. Pour the less viscous part B into the part A container using wood tongue depressor to scoop out all the liquid and mix the two parts for 20 minutes.

7) Pour the mixture in to the mold. Make sure that it’s placed in the center on the mold

8) Insert the lid carefully, excess mixture will come out from all directions

9) Tighten the 4 top screws and put in pressure chamber for 48 hours

(pressure:60psi)

THIS PAGE INTENTIONALLY LEFT BLANK

LIST OF REFERENCES

[1] N. J. Wade and D. Deutsch, “Early binaural research,” *Acoustics Today*, vol. 4, no. 3, pp. 16–27, Jul. 2003. [Online]. Available: http://deutsch.ucsd.edu/pdf/AT-2008_4_3.pdf. Accessed July 12, 2015.

[2] T. R. Letowski and S.T. Letowski, “Auditory spatial perception: Auditory localization,” *Army Research Laboratory*, 2012. [Online]. Available: http://www.dtic.mil/cgi-bin/GetTRDoc?AD=ADA562292. Accessed July 12, 2015.

[3] X. Xiang. (2013, Mar. 13). “How does the brain locate sound sources? [Online]. Available: http://knowingneurons.com/2013/03/15/how-does-the-brain-locate-sound-sources

[4] R. N. Miles, and R. R. Hoy. “The development of a biologically inspired directional microphone for hearing aids,” *Audiol. Neurotol*. vol. 11, no. 2, 86–94 (2006).

[5] H. J. Liu, M. Yu, and X. M. Zhang. “Biomimetic optical directional microphone with structurally coupled diaphragms,” *Appl. Phys. Lett*. 93(24), 243902 (2008).

[6] R. C. Rabelo, F. Alves, and G. Karunasiri, “Electronic phase shift measurement for the determination of acoustic wave DOA using single MEMS biomimetic sensor,” *Scient. Reports,* vol. 10Jul. 2020. [Online]. https://doi.org/10.1038/s41598-020-69563-1

[7] R. N. Miles, Q. Su, W. Cui, and M. Shetye, “A low-noise differential microphone inspired by the ears of the parasitoid fly *Ormia ochracea,” J. Acoust. Soc. Am*. 125(4), 2013–2026 (2009).

[8] M. Tousea, J. Sinibaldi, K. Simsek, J. Catterlin, S. Harrison, and G. Karunasiri. “Fabrication of a microelectromechanical directional sound sensor with electronic readout using comb fingers,” *Appl. Phys. Lett.* 96(17), 173701 (2010).

[9] M. Touse, J. Sinibaldi, and G. Karunasiri. “MEMS directional sound sensor with simultaneous detection of two frequency bands,” *IEEE Sens. Conf.* 1, 2422–2425 (2010).

[10] A. P. Lisiewski, H. J. Liu, L. Currano, and D. Gee, “Fly-ear inspired micro-sensor for sound source localization in two dimensions,” *J. Acoust. Soc. Am.* 129(5), EL166–EL171 (2011).

[11] M. L. Kuntzman, C. T. Garcia, A. G. Onaran, B. Avenson, K. D. Kirk, and N. A. Hall, “Performance and modeling of a fully packaged micromachined optical microphonem,” *J. Microelectromech. Syst*. 20(4), 828–833 (2011).

[12] M. L. Kuntzman, J. G. Lee, N. N. Hewa-Kasakarage, D. Kim, and N. A. Hall, "Micromachined piezoelectric microphones with inplane directivity," *Appl. Phys. Lett.* 102(5), 054109 (2013).

[13] H.Liu, L. Currano, D. Gee, T. Helms, and M. Yu, "Understanding and mimicking the dual optimality of the fly ear," *Nat. Sci. Rep*. 3, 2489 (2013).

[14] M. L. Kuntzman, N. A. Hall, "Sound source localization inspired by the ears of the *Ormia ochracea," Appl. Phys. Lett*. 105(3), 033701 (2014).

[15] R. N. Miles, W. Cui, Q. T. Su, and D. Homentcovschi, "A MEMS low-noise sound pressure gradient microphone with capacitive sensing. *J. Microelectromech. Syst.* 24(1), 241–248 (2015).

[16] D.Wilmott, F.Alves, and G. Karunasiri, "Bio-inspired miniature direction finding acoustic sensor," *Nat. Sci. Rep*. 6, 29957 (2016).

[17] MEMSCAP, "SOIMUMPs and MEMS Multi Project Wafer Service." Accessed October 30, 2016. [Online]. Available: http://www.memscap.com/products/mumps/soimumps/

[18] M. Touse, J. Sinibaldi, K. Simsek, J. Catterlin, S. Harrison, and G. Karunasiri, "Fabrication of a microelectromechanical directional sound sensor with electronic readout using comb fingers," *Appl. Physics Lett*., vol. 96, no. 17, 2010.

[19] B. Gureck, "Resolving bearing ambiguity with a single bio-inspired direction finding microelectromechanical system acoustic sensor," M.S. thesis, Dept. Physics, Naval Postgraduate School, Monterey, CA, June 2020.

[20] R. Miles, D. Robert, and R. Hoy, "Mechanically coupled ears for directional hearing in the parasitoid fly *Ormia Ochracea*," *J. Acoust. Soc. Am.*, vol. 98, no. 6, pp. 3059–3070, Dec. 1995.

[21] A. A. Espinoza Peyrot, "Packaging and characterization of bio-inspired underwater MEMS directional sound sensor," M.S. thesis, Dept. Physics, Naval Postgraduate School, Monterey, CA, June 2019.

[22] D. Wilmott, F. Alves, and G. Karunasiri, "MEMS acoustic directional finding sensor," presented at the *AAAS 2015 Annual Meeting, San Jose, CA*, February 12-16, 2015.

[23] J. Roberts, "Microelectromechanical systems directional acoustic sensor for underwater applications," M.S. thesis, Dept. Physics, Naval Postgraduate School, Monterey, CA, June 2020.

[24] S. L. Ehrlich and P. D. Frelich, "Sonar transducer," U.S. Patent 3290646 Dec. 6, 1966. [Online]. Available: https://patents.google.com/patent/US3290646A/en

[25] S. L. Ehrlich, N. Serotta, and K. Kleinschmidt, “Multimode ceramic transducers,” *The Journal of the Acoustical Society of America*, vol. 31, no. 6, pp. 854–854, Jun. 1959. [Online]. doi: https://doi.org/10.1121/1.1936213

[26] L. L. Beranek and T. J. Mellow, *Acoustics Sound Fields and Transducers*. Oxford: Academic Press, 2012.

[27] F. Edalatfar, S. Azimi, A. Q. Ahsan Qureshi, B. Yaghootkar, W. Friedrich, A. M. Leung, B. Bahreyni, and A. Keast, “A wideband, low-noise accelerometer for sonar wave detection,” *IEEE Sensors Journal*, vol. 18, no. 2, pp. 508–516, Jan. 2018. [Online]. doi: https://doi.org/10.1109/JSEN.2017.2774705

[28] R. Dymond, A. Sapienza, L. Troiano, P. Guerrini, and A. Maguer, “New vector sensor design and calibration measurements,” in *Proc. of the Fourth International Conf. of Underwater Acoustic Measurements: Technologies and Results*, Kos Island, Greece, 2011.

[29] E. German Da Re, “MEMS underwater direction finding acoustic sensor,” M.S. thesis, Dept. Physics, Naval Postgraduate School, Monterey, CA, September 2018.

[30] J. D. Collins, “Bio-inspired MEMS underwater direction finding acoustic sensor,” M.S. thesis, Dept. Physics, Naval Postgraduate School, Monterey, CA, September 2017.

THIS PAGE INTENTIONALLY LEFT BLANK

INITIAL DISTRIBUTION LIST

1. Defense Technical Information Center
   Ft. Belvoir, Virginia

2. Dudley Knox Library
   Naval Postgraduate School
   Monterey, California